JOURNAL OF VIROLOGY, Dec. 2007, p. 13092–13104 Vol. 81, No. 23
0022-538X/07/$08.00+0 doi:10.1128/JVI.01378-07

Varicella-Zoster Virus Modulates NF-κB Recruitment on Selected Cellular Promoters[▽]

Nadia El Mjiyad, Sébastien Bontems, Geoffrey Gloire, Julie Horion, Patricia Vandevenne, Emmanuel Dejardin, Jacques Piette, and Catherine Sadzot-Delvaux*

GIGA-Research, Virology and Immunology Unit, GIGA B34, University of Liège, B-4000 Liège, Belgium

Received 25 June 2007/Accepted 31 August 2007

Intercellular adhesion molecule 1 (ICAM-1) expression is down-regulated in the center of cutaneous varicella lesions despite the expression of proinflammatory cytokines such as gamma interferon and tumor necrosis factor alpha (TNF-α). To study the molecular basis of this down-regulation, the ICAM-1 induction of TNF-α was analyzed in varicella-zoster virus (VZV)-infected melanoma cells (MeWo), leading to the following observations: (i) VZV inhibits the stimulation of *icam-1* mRNA synthesis; (ii) despite VZV-induced nuclear translocation of p65, p52, and c-Rel, p50 does not translocate in response to TNF-α; (iii) the nuclear p65 present in VZV-infected cells is no longer associated with p50 and is unable to bind the proximal NF-κB site of the *icam-1* promoter, despite an increased acetylation and accessibility of the promoter in response to TNF-α; and (iv) VZV induces the nuclear accumulation of the NF-κB inhibitor p100. VZV also inhibits *icam-1* stimulation of TNF-α by strongly reducing NF-κB nuclear translocation in MRC5 fibroblasts. Taken together, these data show that VZV interferes with several aspects of the immune response by inhibiting NF-κB binding and the expression of target genes. Targeting NF-κB activation, which plays a central role in innate and adaptive immune responses, leads to obvious advantages for the virus, particularly in melanocytes, which are a site of viral replication in the skin.

Varicella-zoster virus (VZV) is a human alphaherpesvirus responsible for two diseases. It causes varicella (chicken pox), establishes latency in sensory ganglia, and may reactivate to cause herpes zoster (shingles) in the host (58). VZV enters the host via the respiratory mucosal epithelium, from which it is transported to the skin via a cell-associated viremia (3, 36, 38, 41). It was proposed that melanocytes are the main site of viral replication in the skin prior to the appearance of the typical vesicular lesions (23). Finally, the virus reaches the sensory ganglia, where it may remain latent for years (12, 13, 20, 50).

The innate immune response to VZV seems to be characterized by the production of granulysin by NK cells and of alpha interferon (IFN-α), reducing viral replication (1, 24). In vitro, inflammatory cytokines were also shown to be produced, in a Toll-like receptor 2-dependent manner, by monocytes/macrophages (57). In addition, peripheral blood mononuclear cells from patients with acute varicella infection produce larger amounts of IFN-γ, tumor necrosis factor alpha (TNF-α), and interleukin-12 (IL-12) in vitro than do those from naïve patients, and these cytokines were also shown to be capable of inhibiting viral replication at an early time of infection (29, 54). Furthermore, these cytokines have been detected in the bloodstream of VZV-infected patients, suggesting that they have a crucial role in the control of VZV infection (for reviews, see references 1 and 54). Like many other viruses, VZV evades the immune response in different ways (2, 4, 43). A study on skin biopsies reported that VZV down-regulates intercellular adhesion molecule 1 (ICAM-1; CD54) in infected cells located in the center of cutaneous vesicular lesions, despite the presence of IFN-γ and TNF-α (45), suggesting that the modulation of ICAM-1 expression in response to proinflammatory cytokines could have a major influence on viral replication in skin.

ICAM-1, an 80- to 114-kDa inducible surface glycoprotein, belongs to the immunoglobulin superfamily and is involved in a wide range of immune responses (52). ICAM-1 binds to LFA-1 and Mac-1, two integrins expressed by leukocytes. This interaction promotes cell adhesion and leukocyte extravasation (17, 52). It has also been shown that ICAM-1 expression on nonendothelial cells also plays a key role in the immune response, especially for the activation of $CD8^+$ T cells (39, 40). The *icam-1* promoter contains two putative TATA boxes, two sites for NF-κB, AP-1, AP-2, and the GC receptor element, and one IFN-γ activated site (GAS) (14, 28, 56). ICAM-1 expression can be induced by proinflammatory cytokines such as IL-1β and TNF-α, which stimulate its expression mainly via NF-κB activation (49).

NF-κB consists of two subunits of either homo- or heterodimers of RelA (p65), RelB, c-Rel, NF-κB1 (p105 processed to p50), and NF-κB2 (p100 processed to p52) (25). Most NF-κB complexes are sequestered in the cytoplasm and prevented from activating transcription by proteins referred to as inhibitors of NF-κB or IκB proteins (IκBα, -β, and -ε, p100, and p105). After stimulation, the IκB proteins are phosphorylated by the IκB kinases (IKKs), ubiquitinated, and degraded by the proteasome, allowing nuclear translocation of freed NF-κB (35). Two main pathways leading to NF-κB activation have been described. The classical pathway, activated by proinflammatory cytokines such as TNF-α and IL-1β, leads to IKK complex activation, IκBα degradation, and mostly p50-p65 heterodimer nuclear translocation. On the other hand, the so-

* Corresponding author. Mailing address: GIGA-Research, Virology and Immunology Unit, GIGA B34, University of Liège, B-4000 Liège, Belgium. Phone: 32-4-3663673. Fax: 32-4-3664534. E-mail: csadzot@ulg.ac.be.

▽ Published ahead of print on 12 September 2007.

called alternative pathway, activated by LTβ, BAFF, CD40, and some viruses, leads to p100 processing into p52, which generally translocates with RelB (8, 15, 25, 30, 35). NF-κB possesses the ability to promote the expression of numerous proteins involved in innate and adaptive immunity and thus regulates the immune response following various stimuli, including infections. Several viruses, herpesviruses in particular, have developed strategies to interfere with NF-κB activation in order to evade the immune response or to activate it for their own interest (5, 6, 42). A microarray analysis of VZV-infected fibroblasts revealed that several NF-κB-dependent genes were down-regulated during VZV infection (31), and it was recently shown that VZV inhibits NF-κB translocation in infected fibroblasts (30), but not much is known about the molecular basis of this NF-κB inhibition in VZV-infected cells.

Since a down-regulation of ICAM-1 was observed in VZV-induced skin lesions despite the presence of TNF-α, we studied the inhibition of ICAM-1 stimulation by TNF-α in VZV-infected human melanoma cells (MeWo) and human fibroblasts (MRC5). We demonstrate in this paper that this inhibition occurs at the transcriptional level, since the *icam-1* mRNA was not synthesized in VZV-infected cells. We also show by electrophoretic mobility shift assay (EMSA) that the nuclear NF-κB subunits present in VZV-infected cells are unable to bind the NF-κB site on the *icam-1* promoter following TNF-α treatment. We also highlight the observation that despite a steady-state level of p65, this subunit was drastically less associated with p50 in VZV-infected MeWo cells. Using coimmunoprecipitation experiments, we demonstrate that both p65 and p50 are more associated with p100 in VZV-infected MeWo cells. Moreover, using chromatin immunoprecipitation (ChIP) assays of MeWo cells, we highlight that the recruitment of the NF-κB subunits p50, p65, and p52 to the *icam-1* promoter upon TNF-α treatment is strongly inhibited by infection. This inhibition occurs while both protein and mRNA levels of IκBα are already very low. The inhibition of the NF-κB pathway is specific, since the STAT-1 activation pathway was intact in VZV-infected MeWo cells. We concluded that VZV specifically inhibits the NF-κB activation pathway by destabilizing p65-p50 heterodimers and increasing their cytoplasmic association with p100.

MATERIALS AND METHODS

Cell culture and viruses. The human melanoma cell line MeWo and the fibroblast cell line MRC5 were cultured in Eagle's minimal essential medium (Biowhitaker, Petit-Rechain, Belgium) supplemented with 10% fetal bovine serum, 1% glutamine, and 1% nonessential amino acids (GIBCO, Merelbeke, Belgium). We used the VZV strain rOKA-gfp, a recombinant strain expressing the *gfp* gene under the control of the cytomegalovirus immediate-early promoter, to infect MeWo cells and the VZV strain rOKA, which does not express green fluorescent protein (a kind gift from Marvin Sommer) (59), to infect MRC5 cells. The cells were infected by coculture with infected cells at a ratio of 1 to 10.

Protein extraction, EMSAs, and supershift experiments. Nuclear and cytoplasmic extraction and gel shift experiments were performed as previously described (55), using either a probe carrying the proximal NF-κB sequence of the human *icam-1* promoter or the κB sequence of the human immunodeficiency virus (HIV) long terminal repeat (LTR) promoter. The supershift experiments were performed by incubating 5 μg of nuclear proteins with 2 μg of antibody for 20 min prior to reaction with a DNA probe (for p65, sc109x; for p50, sc1191x; for cRel, sc6955x; for RelB, sc226x; and for p52, sc7386x [Tebu Bio, CA]).

Western blotting. Twenty micrograms of cytoplasmic or nuclear extract was incubated with sodium dodecyl sulfate (SDS) loading buffer (10 mM Tris-HCl, pH 6.8, 1% SDS, 25% glycerol, 0.1 mM β-mercaptoethanol, and 0.03% bromophenol blue), boiled for 3 min, and subjected to SDS-polyacrylamide gel electrophoresis. After transfer to a polyvinylidene fluoride membrane (Roche Applied Sciences, Basel, Switzerland) and blocking with PBS-Tween containing 5% dry milk, the membrane was incubated at room temperature under agitation with different antibodies, including antibodies to ICAM-1, p105/p50, and p65 (Tebu Bio, CA); actin (Sigma, Bornem, Belgium); RelB, c-Rel, p100/p52, and Nijmegen breakage syndrome (NBS) (Upstate Cell Signaling, Charlottesville, VA); and IκBα (kindly provided by R. Hay, St. Andrews, Scotland).

Coimmunoprecipitation assays. Cells were lysed in 300 μl of immunoprecipitation buffer (25 mM HEPES, 150 mM NaCl, 0.5% Triton, 10% glycerol, 1 mM dithiothreitol, 1 mM Na_3VO_4, 25 mM β-glycerophosphate, 1 mM NaF, Complete, 1 mM nitrophenyl phosphate). One milligram of total cell extract was incubated overnight in 1 ml of immunoprecipitation buffer with 2 μg of antibody (for p65, sc-109 [Tebu Bio, CA]; for p50, 06-886 [Upstate Cell Signaling, Charlottesville, VA]; for p52/p100, 06-413 [Upstate Cell Signaling, Charlottesville, VA]; and for hemagglutinin, 1867423 [Roche Applied Sciences, Basel, Switzerland]). The cell lysate and the antibody were then incubated for 2 h with protein G-agarose beads (SPA-806; Stressgene). The beads were washed three times in the immunoprecipitation buffer. The beads were then incubated with 30 μl of 2% SDS for 10 min at 37°C and centrifuged at 14,000 rpm for 1 min. The eluted proteins were incubated with the SDS loading buffer, boiled for 3 min, and subjected to SDS-polyacrylamide gel electrophoresis. Western blot analysis was used to detect the coimmunoprecipitated proteins.

The same protocol was used for coimmunoprecipitation in nuclear extracts, except that 500 μg of nuclear extract was incubated in 1 ml of immunoprecipitation buffer.

mRNA expression studies. Total RNAs were extracted and cDNAs prepared as previously described (55). Two microliters of cDNA was subjected to quantitative PCR using the SYBR green mix method (Applied Biosystems, Warrington, United Kingdom). The following primers were used: for *icam-1*, FW (5′-GCAGACAGTGACCATCTACAGCTT-3′) and RV (5′-CTTCTGAGACC TCTGGCTTCGT-3′); for *il-8*, FW (5′-GAAGGAACCATCTCACTGTGTGT AA-3′) and RV (5′-ATCAGGAAGGCTGCCAAGAG-3′); for *iκbα*, FW (5′-C CAACCAGCCAGAAATTGCT-3′) and RV (5′-TCTCGGAGCTCAGGATCA CA-3′); and for *18S*, FW (5′-AACTTTCGATGGTAGTCGCCG-3′) and RV (5′-CCTTGGATGTGGTAGCCGTTT-3′).

ChIP assays. ChIP assays were carried out according to the Upstate Cell Signaling protocol. Protein A-agarose beads were saturated with herring sperm DNA (Sigma-Aldrich, Bornem, Belgium) at 1 μg DNA/20 μl protein A-agarose. All ChIP assays were performed at least three times. Quantitative PCR targeting the promoter region of each gene was performed on the immunoprecipitated DNA. The following primers were designed using the software Primer Express: for *icam-1*, FW (5′-CCCGATTGCTTTAGCTTGGAA-3′) and RV (5′-CCGG AACAAATGCTGCAGTTAT-3′); and for *il-8*, FW (5′-GCCATCAGTTGCAA ATCGTG-3′) and RV (5′-AGTGCTCCGGTGGCTTTT-3′). As a control of binding specificity, we amplified a noncoding region downstream of the albumin gene (as previously described [37]). For specific binding to the beads, treated cell extracts were incubated with 2 μg of irrelevant antibody (anti-Flag). The following antibodies were used: antibodies to p65, p50, histone H3 acetylated at K9, histone H3 acetylated at S10, p52 (Upstate Cell Signaling, Charlottesville, VA), and histone H3 (Abcam, Cambridge, United Kingdom).

Western blot quantification. Quantification was achieved by quantifying the densities of the bands obtained by Western blotting, using the program Quantity One (Bio-Rad Laboratories Inc.).

RESULTS

ICAM-1 is not induced by TNF-α in VZV-infected cells. Since ICAM-1 was shown to be down-regulated in the center of VZV cutaneous lesions while proinflammatory cytokines were present (45), the basis of this down-regulation in VZV-infected cells was investigated. A human melanoma cell line (MeWo) infected with the VZV strain rOka labeled with green fluorescent protein, allowing follow-up of the infection, was used. At 24 and 36 h postinfection, 50 and 90% of the MeWo cells, respectively, were infected. Cells were then treated for 24 h with TNF-α (500 U/ml), a proinflammatory cytokine known to induce ICAM-1 expression, mostly via the NF-κB classical activation pathway (49). ICAM-1 expression was detected by Western blot analysis of total cell lysates. TNF-α induced ICAM-1 expression in mock-infected

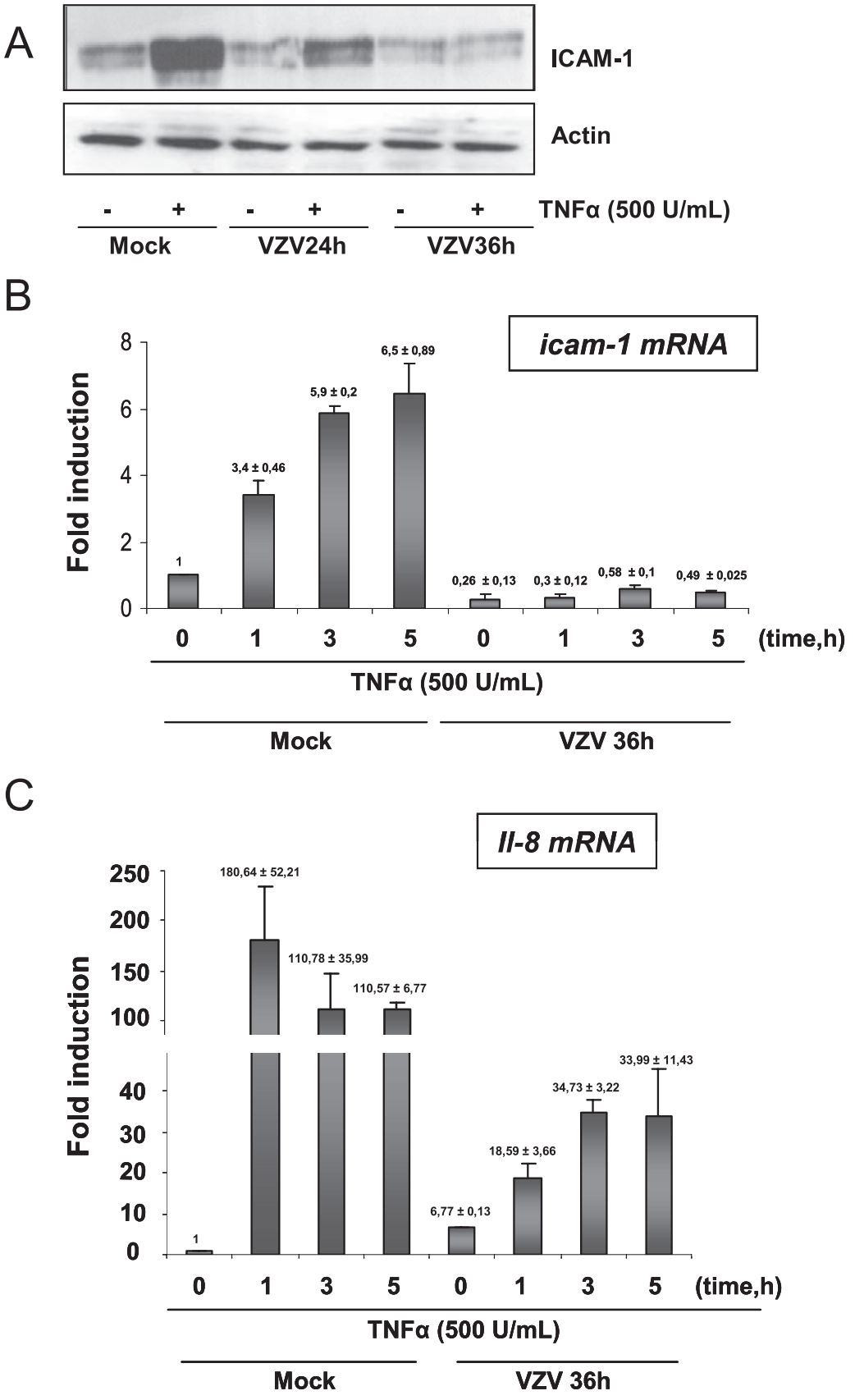
A
ICAM-1
Actin
- + - + - + TNFα (500 U/mL)
Mock
VZV24h
VZV36h
B
icam-1 mRNA
Fold induction
8
6
4
2
0
1
3,4 ± 0,46
5,9 ± 0,2
6,5 ± 0,89
0,26 ± 0,13
0,3 ± 0,12
0,58 ± 0,1
0,49 ± 0,025
0 1 3 5 0 1 3 5 (time,h)
TNFα (500 U/mL)
Mock
VZV 36h
C
Il-8 mRNA
Fold induction
250
200
150
100
40
30
20
10
0
1
180,64 ± 52,21
110,78 ± 35,99
110,57 ± 6,77
6,77 ± 0,13
18,59 ± 3,66
34,73 ± 3,22
33,99 ± 11,43
0 1 3 5 0 1 3 5 (time,h)
TNFα (500 U/mL)
Mock
VZV 36h

cells, but the induction was strongly reduced in VZV-infected cells as early as 24 h postinfection and totally inhibited when cells were treated at 36 h postinfection (Fig. 1A). Similar results were observed using IL-1β, another proinflammatory cytokine also known to stimulate ICAM-1 expression via NF-κB activation (49) (data not shown). It can be concluded that VZV-infected cells do not respond to proinflammatory cytokine-induced ICAM-1 expression, mimicking the situation described for skin lesions (45).

***icam-1* gene transcription is down-regulated in VZV-infected cells treated with TNF-α.** Quantitative reverse transcription-PCR (RT-PCR) was used to determine whether *icam-1* mRNA synthesis was induced in VZV-infected MeWo cells in response to TNF-α (18S RNA was used as an internal control). As shown in Fig. 1B, VZV reduced the basal level of *icam-1* gene expression (0 h). As expected, TNF-α (500 U/ml) up-regulated *icam-1* gene transcription up to sixfold as early as 3 h after treatment of mock-infected cells, while *icam-1* gene transcription was not induced in VZV-infected cells. To ensure that these observations were not due to a destabilization of the mRNA, the stability of *icam-1* mRNA was measured by treating cells with a transcription inhibitor, actinomycin D (5 μg/ml), and the transcript half-lives in mock- and VZV-infected cells were compared. The *icam-1* mRNA half-lives in both mock- and VZV-infected cells were quite similar, at around 30 min (data not shown). In conclusion, VZV does not alter the mRNA stability but inhibits ICAM-1 expression in response to TNF-α by inhibiting its transcription.

Since the basal level of expression of the *icam-1* gene was already lowered by the VZV infection, we could not exclude the possibility that there was a general shutoff of the cellular promoters. We then investigated whether the *il-8* gene, an NF-κB-dependent gene that was not down-regulated upon infection, could respond to TNF-α in VZV-infected cells. *il-8* gene transcription following TNF-α treatment was induced up to 180-fold after 1 hour of TNF-α treatment in mock-infected cells (Fig. 1C). Interestingly, VZV infection alone was able to up-regulate *il-8* gene transcription up to 7-fold, and this up-regulation was further increased, up to 34-fold, in VZV-infected cells after TNF-α treatment (500 U/ml). Yet even if the *il-8* promoter still responded to TNF-α treatment, the induction was very weak compared to that in mock-infected cells, and it rapidly reached a plateau, meaning that there was still a limiting factor induced by VZV infection. Altogether, these data show that VZV infection is able to interfere with or even to inhibit the transcription of NF-κB-dependent genes in response to TNF-α.

In vitro, NF-κB DNA-binding ability is specifically inhibited in VZV-infected cells. The *icam-1* promoter contains two putative TATA boxes, two sites for NF-κB, AP-1, AP-2, and the GC receptor element, and one site for GAS (14, 28, 56). While the distal NF-κB site seems to be dispensable, the proximal

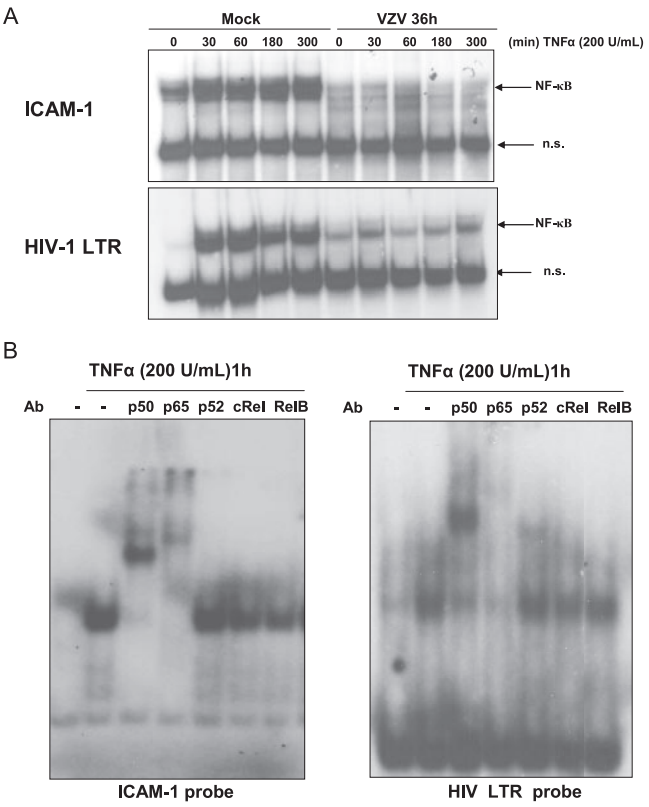

FIG. 2. NF-κB binding ability is inhibited by VZV infection. (A) MeWo cells were either mock or VZV infected for 36 h prior to treatment with TNF-α (200 U/ml) for increasing times. Nuclear extracts were harvested. The nuclear extracts were used to study NF-κB activation by EMSA, using a radiolabeled probe carrying the sequence of the *icam-1* promoter's proximal NF-κB site (top) or the HIV LTR promoter NF-κB sequence (bottom). (B) The NF-κB subunits involved in binding were characterized by supershift experiments. MeWo cells not infected by VZV were treated with TNF-α, and nuclear extraction was performed. The nuclear extracts were incubated with antibodies directed against every NF-κB subunit before starting the EMSA. n.s., nonspecific.

one has a major role in the response to proinflammatory cytokines, such as TNF-α, IL-1β, and IFN-γ (49). TNF-α and IL-1β activate NF-κB via the classical pathway, inducing the degradation of IκBα and thus releasing p50-p65 heterodimers (25). The binding of this dimer to the proximal NF-κB site within the *icam-1* promoter is essential and sufficient to trigger transcription activation in response to TNF-α (56).

Nuclear NF-κB binding to the *icam-1* proximal NF-κB site was investigated in mock- and VZV-infected cells by mobility shift assay. As shown in Fig. 2A (upper panel), TNF-α induced NF-κB binding to the *icam-1* probe as early as 30 min in

FIG. 1. ICAM-1 is not induced by TNF-α treatment in VZV-infected cells. (A) MeWo cells infected with VZV for 24 and 36 h were treated with TNF-α (500 U/ml) for 24 h. Total cell lysates were harvested, and the level of ICAM-1 was analyzed by Western blotting. After 24 h, 50% of the MeWo cells were infected, and after 36 h, 80 to 90% of the cells were infected. The actin expression level was used as a loading control. (B) MeWo cells were mock or VZV infected for 36 h and treated for increasing times with TNF-α (500 U/ml). *icam-1* mRNA expression was analyzed by quantitative RT-PCR and normalized using the 18S RNA level. (C) MeWo cells were either mock or VZV infected for 36 h before being treated with TNF-α (500 U/ml) for increasing times. Total RNA extracts were isolated and analyzed by real-time RT-PCR, using primers for the *il-8* mRNA. RT-PCR was normalized using the 18S RNA expression level.

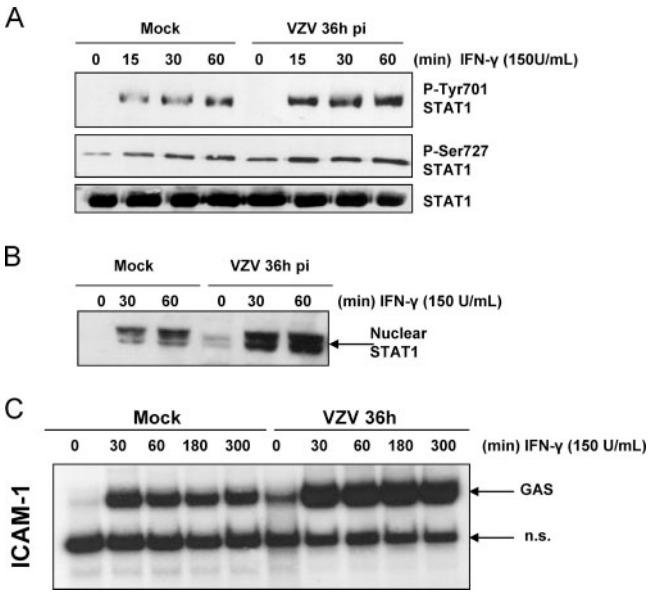

FIG. 3. The STAT-1 activation pathway is not inhibited at 36 h postinfection. (A) Mock- and VZV-infected cells were treated with IFN-γ for increasing times. STAT-1 was then immunoprecipitated from total cell lysates. The phosphorylation on Y701 and S727 was analyzed by Western blotting. A Western blot against STAT-1 was performed as a loading control. (B) Nuclear extracts were harvested from mock- and VZV-infected cells treated with IFN-γ for 30 and 60 min. Western blot analysis was carried out using an antibody directed against STAT-1. (C) MeWo cells were either mock or VZV infected for 36 h prior to treatment with IFN-γ (150 U/ml) for increasing times. Nuclear extracts were harvested and analyzed for STAT-1 activation by EMSA, using a radiolabeled probe carrying the sequence of the *icam-1* promoter GAS site. n.s., nonspecific.

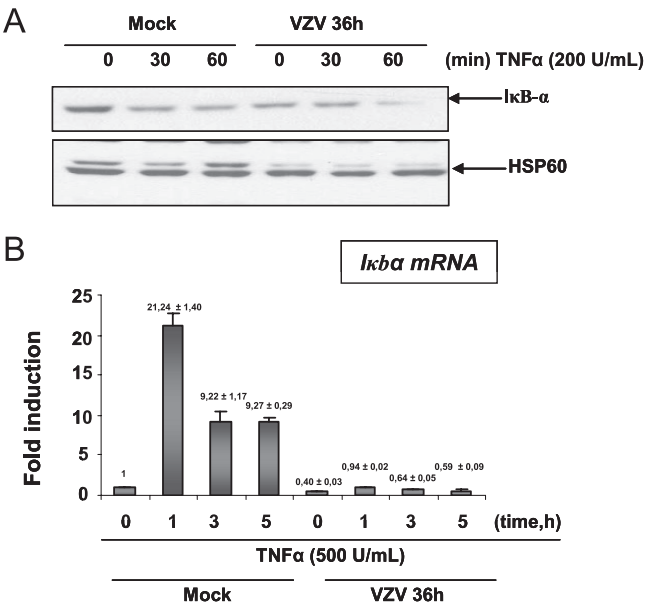

FIG. 4. IκBα level is lowered at late times of infection. (A) MeWo cells were either mock or VZV infected for 36 h prior to treatment with TNF-α (200 U/ml) for increasing times. The cytoplasmic extracts were harvested and used for Western blot analysis of IκBα protein expression. A Western blot of the HSP60 protein was used as a loading control. (B) MeWo cells were either mock or VZV infected for 36 h before treatment for increasing times with TNF-α (500 U/ml). Total RNA extracts were isolated and analyzed by real-time RT-PCR, using primers for *ikbα* mRNA. RT-PCR was normalized using the 18S RNA expression level.

mock-infected MeWo cells, whereas this binding was completely inhibited in VZV-infected cells. It should also be noted that the basal level of NF-κB binding on the *icam-1* probe was also reduced by the infection. The binding of NF-κB to another probe, carrying the NF-κB binding sequence of the HIV LTR promoter, was also tested in order to see whether the inhibition was specific to the *icam-1* promoter. While VZV totally inhibited the NF-κB binding on the *icam-1* probe, it less severely inhibited binding to the HIV probe (Fig. 2A, lower panel). Finally, a supershift experiment using antibodies directed against the different NF-κB subunits was carried out. As shown in Fig. 2B, p65 and p50 were the main subunits binding the *icam-1* and HIV probes in response to TNF-α.

Mock- and VZV-infected cells were then treated with IFN-γ to check STAT-1 activation in order to ensure that NF-κB inhibition was specific. As shown in Fig. 3, not only was STAT-1 still phosphorylated on both Y701 and S727 (Fig. 3A), but it translocated to the nuclei of VZV-infected cells in response to IFN-γ (Fig. 3B) and was still able to bind a probe carrying the GAS sequence of the *icam-1* gene (Fig. 3C). Interestingly, binding to the GAS probe was increased upon VZV infection. These experiments clearly highlighted the VZV-specific inhibition of NF-κB activation while the cells were still able to mount a normal STAT-1 activation.

IκBα expression is reduced in VZV-infected cells at late times of infection. IκBα is the cytoplasmic inhibitor of NF-κB. Western blot analysis revealed that in mock-infected cells, TNF-α induced a transient degradation of IκBα, while in VZV-infected MeWo cells, the basal level of IκBα protein was already very low and slightly decreased after 1 h of TNF-α treatment (Fig. 4A). The *iκbα* transcription level analyzed by quantitative RT-PCR revealed that mRNA synthesis was no longer induced by TNF-α in VZV-infected cells (Fig. 4B). Moreover, the basal level of expression of this gene was reduced by VZV infection. Altogether, these data suggest that VZV infection inhibits IκBα neosynthesis.

VZV infection impairs p50 but not p65 nuclear translocation. In order to determine whether the VZV-induced inhibition of NF-κB binding in the presence of TNF-α was due to a cytoplasmic retention of some or all NF-κB components, the intracellular localization of the different NF-κB subunits was analyzed by Western blotting of nuclear and cytoplasmic extracts. As shown in Fig. 5A (panel 1), p65 translocated into the nuclei of mock-infected cells upon TNF-α treatment. VZV by itself led to p65 translocation, as indicated by the high basal level of p65 in the nuclei of untreated infected cells (0 min). However, the amount of nuclear p65 was not increased any further by TNF-α. p50 analysis revealed its correct nuclear translocation in mock-infected cells upon TNF-α treatment, while its basal level was not increased in infected cells and was maintained low upon TNF-α induction (Fig. 5A, panel 2). From these observations, it appears that VZV infection promotes the nuclear translocation of p65 independently of p50. It is interesting that while the level of IκBα was already low in VZV-infected cells, p50-containing dimers still failed to translocate into the nucleus.

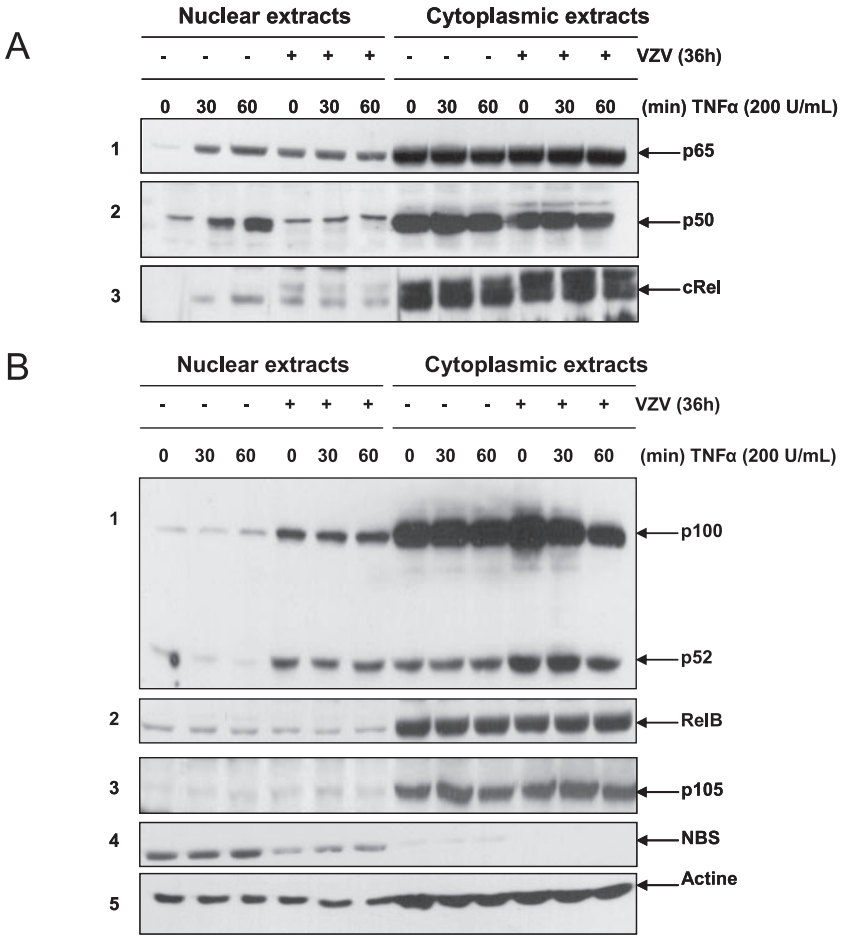

FIG. 5. Nuclear translocation of NF-κB subunits is disrupted by VZV infection of MeWo cells. MeWo cells were either mock or VZV infected for 36 h prior to treatment with TNF-α (200 U/ml) for increasing times. The nuclear and cytoplasmic levels of various NF-κB subunits, activated mostly via the classical NF-κB activation pathway (p65, p50, and c-Rel) (A) or the alternative pathway (p100, p52, and RelB) (B), were analyzed by Western blotting. Nuclear and cytoplasmic contaminations were evaluated using anti-p105 and anti-NBS antibodies, respectively. Actin was used as a loading control.

The analysis of the other NF-κB subunits revealed that c-Rel nuclear translocation was observed in mock-infected cells treated with TNF-α, while VZV infection led to a basal level of c-Rel which was significantly higher than that in mock-infected cells and did not increase in response to TNF-α (Fig. 5A, panel 3). Therefore, c-Rel behaves rather similarly to p65. Nevertheless, this study was not pursued any further since it appeared that c-Rel does not bind the *icam-1* promoter upon TNF-α treatment (Fig. 2B).

Other NF-κB subunits, such as p100/p52 and RelB, were also analyzed. Interestingly, nuclear levels of both p100 and p52 were strongly increased in VZV-infected cells but were not modified by TNF-α treatment (Fig. 5B, panel 1). No clear differences in the nuclear level of RelB between mock- and VZV-infected cells, either treated or not with TNF-α, were detected (Fig. 5B, panel 2). p105, an exclusively cytoplasmic protein, and NBS, an exclusively nuclear protein, were used as quality controls (Fig. 5B, panels 3 and 4). An anti-actin Western blot analysis was also done to control gel loading (Fig. 5B, panel 5).

VZV destabilizes p50, reducing the occurrence of p50-associated p65. Since p65-p50 heterodimers are critical for TNF-α-induced *icam-1* transcription (51), the extent to which the NF-κB subunits interact with each other was investigated by immunoprecipitation of mock- and VZV-infected cells. As shown in Fig. 6A (lanes 1 and 2), p65 was significantly less associated with p50 in VZV-infected MeWo cells than in uninfected cells. While its association with p52 was not influenced by infection, p65 seemed slightly more associated with the inhibitor p100 in VZV-infected cells. Concerning p50-containing complexes (Fig. 6A, lanes 3 and 4), it seemed that the p50 remaining in the VZV-infected cells was still associated with p65 and p52, while p50 seemed slightly more associated with p100. Finally, p100 and p52 were immunoprecipitated (Fig. 6A, lanes 5 and 6). For equal amounts of these subunits, equivalent amounts of p65 and p50 were coimmunoprecipitated in mock- and VZV-infected cells.

Finally, p65 was immunoprecipitated from nuclear extracts of TNF-α-treated mock- and VZV-infected MeWo cells (Fig. 6B). It turned out that the nuclear p65 in VZV-infected cells

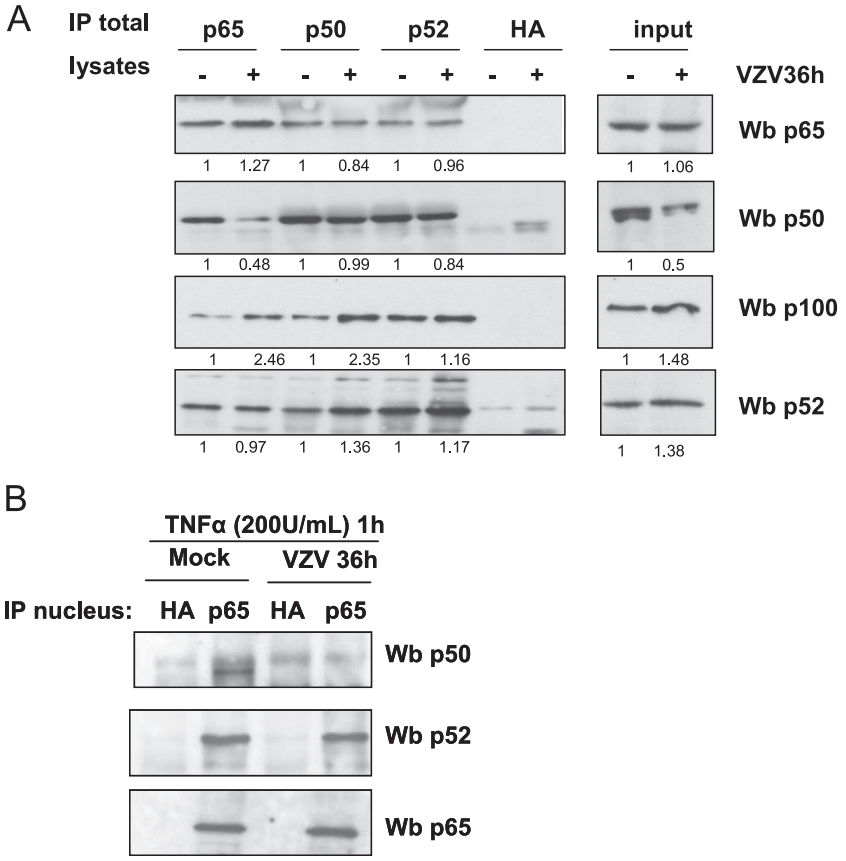

FIG. 6. VZV destabilizes p65-p50 heterodimers and increases their p100 association. (A) Total cell extracts from mock- and VZV-infected MeWo cells were incubated overnight with 2 μg of antibodies directed against p65, p50, and p100/p52. An antibody directed against hemagglutinin (HA) was used to control the specificity of the immunoprecipitation (IP). A Western blot (Wb) analysis was used to identify the complexes present in the cells. The results were quantified using Quantity One software from Bio-Rad. The mean value is presented under each band. The results were quantified by considering the mock-infected cell value as 1. (B) Nuclear extracts were made from mock- and VZV-infected MeWo cells treated with TNF-α for 1 h. p65 was then immunoprecipitated from these nuclear extracts, and Western blot analysis was used to identify the p65-associated subunits.

was no longer associated with a detectable amount of p50. With this dimer being the most important for *icam-1* gene stimulation by TNF-α treatment (14, 49, 51), it could be envisioned that its destabilization by the VZV infection strongly compromised *icam-1* transcription induced by TNF-α. In addition, it should be mentioned that an equivalent amount of p52 was coimmunoprecipitated with p65, while p100 could not be coimmunoprecipitated with p65 from the same nuclear extracts (data not shown).

VZV-infected fibroblasts also show an inhibition of NF-κB nuclear translocation. Recently, it was shown that VZV induced IκBα stabilization in fibroblasts at the beginning of the infection, with a cytoplasmic retention of both p65 and p50 (30). In order to compare our results to these data, experiments were repeated with MRC5 fibroblasts infected with the VZV strain rOka. VZV-infected MRC5 cells did not respond to TNF-α (Fig. 7A). Indeed, ICAM-1 synthesis was inhibited as early as 24 h postinfection. Band shift assays were also carried out on nuclear extracts from mock- and VZV-infected cells and clearly showed that NF-κB binding upon TNF-α treatment was as inhibited by infection in MRC5 cells as it was in MeWo cells, even though the basal level of binding was not affected by the infection (Fig. 7B). Finally, cell fractionation was carried out, and p65, p50, p52, and p100 nuclear translocation was analyzed. As shown in Fig. 7C, p65 nuclear translocation increased as much in VZV-infected MRC5 cells as it did in MeWo cells. Nevertheless, the nuclear p65 level was slightly lower than that in the nuclei of TNF-α-treated mock-infected cells. We also observed a slight increase of p50 which was not observed in MeWo cells. p100 and p52 also increased in VZV-infected MRC5 nuclei. It is interesting that TNF-α induced the nuclear translocation of p52 in mock-infected MRC5 cells but not in VZV-infected cells. Thus, it turned out that despite some differences between the two cell lines considered, the virus inhibited NF-κB induction of *icam-1* in both MeWo and MRC5 cells.

VZV perturbs TNF-α-induced NF-κB binding to a specific promoter in vivo. To go one step further into the mechanism by which VZV impairs ICAM-1 inducibility by TNF-α, ChIP assays were carried out with MeWo cells to compare the in vivo recruitment of p50, p65, and p52 to the *icam-1* and *il-8* promoters. Cells infected for 36 h were treated for 60 min with TNF-α (200 U/ml). After ChIP assays using specific antibodies against p50, p52, and p65, quantitative PCR am-

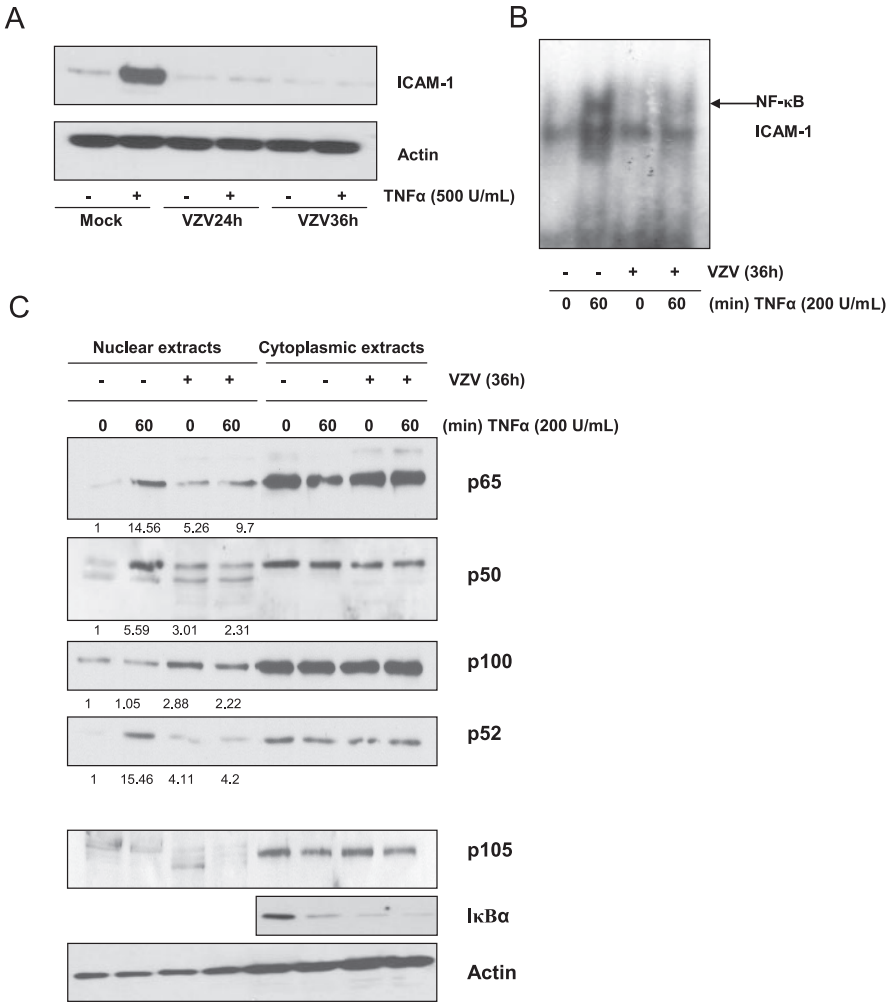

FIG. 7. VZV-infected fibroblasts also show inhibition of NF-κB nuclear translocation. (A) MRC5 cells infected with the VZV strain rOka for 24 and 36 h were treated with TNF-α (500 U/ml) for 24 h. Total cell lysates were harvested, and the level of ICAM-1 was analyzed by Western blotting. Actin was used as a loading control. (B) MRC5 cells were either mock or VZV infected for 36 h prior to treatment with TNF-α (200 U/ml) for increasing times. The nuclear extracts were incubated with a radiolabeled probe carrying the sequence of the *icam-1* promoter proximal NF-κB site. (C) MRC5 cells were either mock or VZV infected for 36 h prior to treatment with TNF-α (200 U/ml) for increasing times. The nuclear and cytoplasmic levels of various NF-κB subunits (p65, p50, and p100/p52) were analyzed by Western blotting. The nuclear translocation of the different NF-κB subunits was quantified using Quantity One software from Bio-Rad, and the mean value is shown under each band. The results were quantified by considering the quantity of subunits present in mock-infected untreated cells as 1. The IκBα protein level was also evaluated in this cell line. Nuclear contamination was assessed with anti-p105, and actin was used as a loading control.

plification of a 100-bp region surrounding the proximal NF-κB site of the *icam-1* promoter was carried out. Immunoprecipitation using an irrelevant antibody (anti-Flag) as well as a PCR with primers amplifying a noncoding region downstream of the *albumin* gene was used as a specificity control (data not shown). As shown in Fig. 8A, TNF-α treatment induced p65 recruitment to the proximal NF-κB site of the *icam-1* promoter in mock-infected cells, while it was not recruited in VZV-infected cells. The basal level of p65 at the promoter was not significantly increased by infection, despite the fact that, as shown above, the nuclear p65 level was increased in VZV-infected cells (Fig. 5A, panel 1). The level of p50 present at the promoter did not significantly increase after TNF-α treatment. The basal level of p50 on the *icam-1* promoter was significantly lower in VZV-infected cells than in mock-infected cells. Finally, neither TNF-α treatment nor VZV infection significantly modulated p52 recruitment to the *icam-1* promoter (Fig. 8A, bottom panel).

Unlike the case for *icam-1*, there was still a slight recruitment of p65 to the *il-8* promoter in VZV-infected cells after TNF-α treatment (Fig. 8B, top panel). In VZV-infected cells, p50 was not recruited to the *il-8* promoter upon TNF-α treatment, and its level was even lower than that in mock-infected cells (Fig. 8B, middle panel). p52 recruitment also showed that it was removed from the *il-8* promoter following TNF-α treatment or VZV infection (Fig. 8B, bottom panel). We could therefore postulate that despite the VZV-induced increased nuclear levels of several NF-κB subunits (p65, c-Rel, and p52), infection abrogates p50/p65 recruitment to the *icam-1* promoter, thereby explaining the loss of response of this gene to TNF-α.

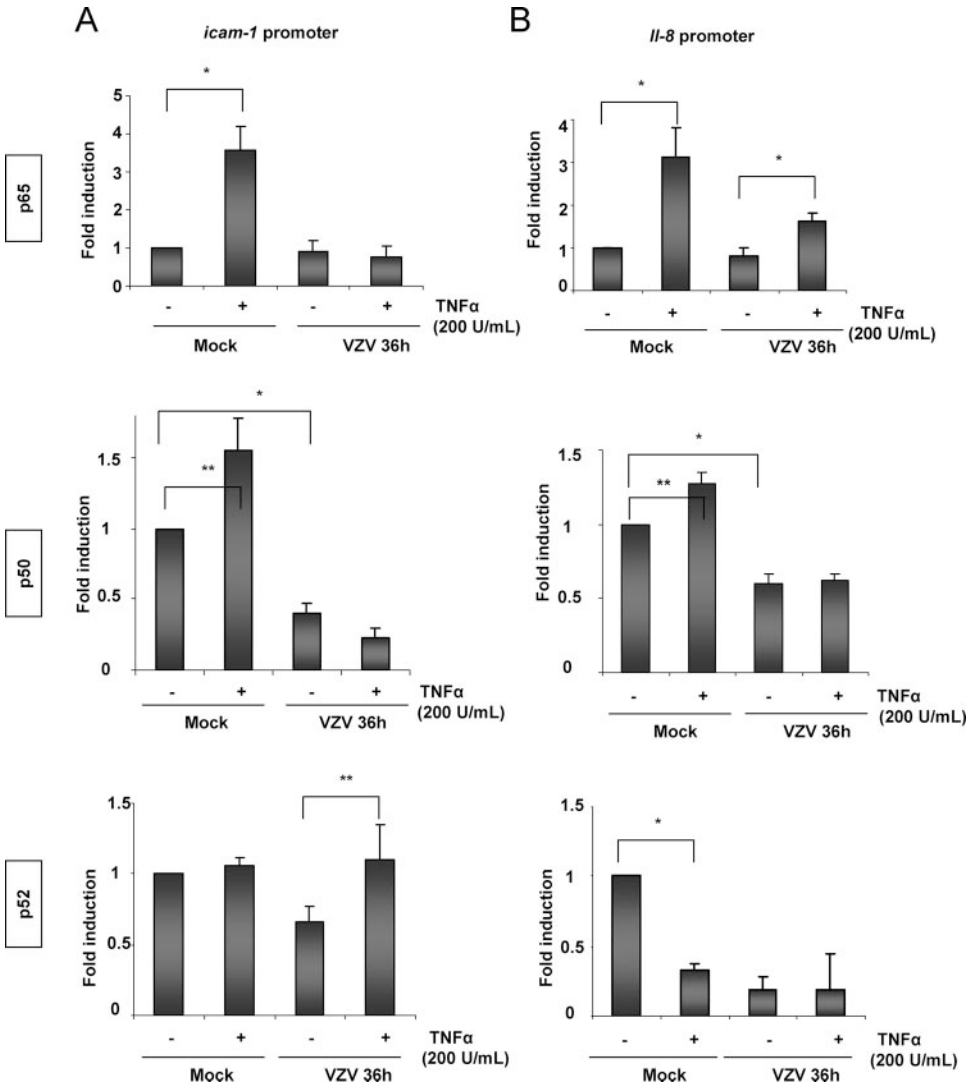

FIG. 8. VZV perturbs NF-κB binding induced by TNF-α on the targeted promoters in vivo. Mock- and VZV-infected MeWo cells were treated for 1 h with TNF-α (200 U/ml), and ChIP assays using p65, p50, or p52 antibody were carried out on total cell lysates. Real-time PCR amplification of a 100-bp fragment from the *icam-1* (A) or *il-8* (B) promoter encompassing the proximal NF-κB site was carried out. The results were normalized by performing PCR on the DNA input. *, statistically different ($P < 0.05$); **, not statistically different ($P > 0.05$).

VZV does not inhibit *icam-1* and *il-8* promoter region acetylation. Histone acetylation and histone deacetylase (HDAC) removal are often correlated with increased chromatin accessibility at NF-κB-responsive promoters (27). Promoter availability was evaluated by analyzing histone H3 acetylation on K9 and the presence of HDAC3 on the promoters of the *icam-1* and *il-8* genes in MeWo cells. As shown by ChIP analysis in Fig. 9, there was an increase in the acetylated histone H3 level at the *icam-1* and *il-8* promoters after TNF-α treatment in mock-infected cells. VZV alone induced an increased acetylation of these promoters, which was further enhanced by TNF-α (Fig. 9A). The experiment was normalized by performing a ChIP assay using an anti-histone H3 antibody. By ChIP assay, the HDAC3 level was shown to be decreased at the *icam-1* and *il-8* promoters after both TNF-α treatment and VZV infection, which correlates with the increased acetylation (Fig. 9B).

From these data, it can be concluded that VZV inhibited NF-κB recruitment to the *icam-1* promoter region and, to a lesser extent, to the *il-8* promoter after TNF-α treatment. The inhibition was observed both in vitro and in vivo, although VZV did not inhibit promoter acetylation, which appeared to be enhanced.

DISCUSSION

In this work, it was demonstrated for the first time that VZV is able to inhibit the expression of ICAM-1 in response to proinflammatory cytokines in infected melanoma cells and fibroblasts. ICAM-1 has a crucial role in different aspects of the immune response. Expressed on endothelial cells, ICAM-1 allows the migration of leukocytes to inflammation sites, while its expression on antigen-presenting cells gives costimulatory signals and plays a crucial role in $CD8^+$ T-cell activation (40). ICAM-1 is poorly expressed in skin cells, but its expression

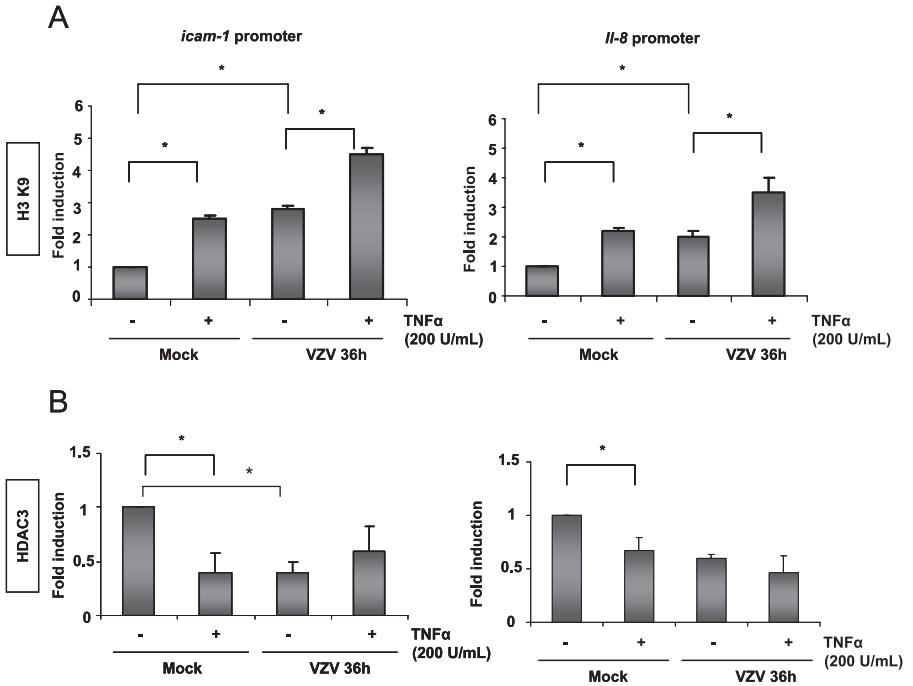

FIG. 9. VZV does not shut off the *icam-1* and *il-8* promoter regions. ChIP assay analysis was carried out on mock- and VZV-infected MeWo cells, using an antibody specific for the K9-acetylated form of histone H3, normalized using an anti-H3 ChIP assay (A), or an antibody specific for HDAC3 (B). The immunoprecipitated DNA was subjected to PCR analysis using primers amplifying the promoter region of either *icam-1* or *il-8*. *, statistically different ($P < 0.05$); **, not statistically different ($P > 0.05$).

level can be up-regulated by proinflammatory cytokines such as IFN-γ or TNF-α, as is the case in the periphery of VZV cutaneous lesions, where the viral load is low. On the other hand, in the center of the lesions, where cells support a high viral load, ICAM-1 is not up-regulated in response to proinflammatory cytokines (45). These cutaneous sites bear a high level of viral replication (7). Diminishing immune surveillance at these sites might allow the virus to replicate more efficiently.

The most interesting feature beyond the down-regulation of ICAM-1 expression is that this inhibition actually specifically targets NF-κB, a transcription factor having a central role in the activation pathways of several genes. Indeed, the NF-κB activation pathway was inhibited, while STAT-1 was normally activated at 36 h postinfection (Fig. 3).

While IκBα protein has been demonstrated to be stabilized at short times of infection in VZV-infected fibroblasts (30) and HEK293 cells (data not shown), we observed a decrease in IκBα protein level in both MeWo and MRC5 cells at late times of infection. IκBα protein has a short turnover time (between 30 and 180 min) (26), and since VZV decreased the basal level of *iκbα* mRNA, this probably led to the decreased IκBα protein level observed in both melanoma cells and fibroblasts at late times of infection. Furthermore, VZV inhibited its TNF-α-induced resynthesis. The NF-κB subunits (p65, c-Rel, and p52) present in the nuclei of VZV-infected cells were shown to be unable to bind the studied promoters. Our results for fibroblasts show that the nuclear translocation of p50 and, to a lesser extent, p65 is strongly decreased by VZV infection. Nevertheless, there is still a p65 nuclear translocation induced by infection, but it never reaches the level observed in mock-infected TNF-α-treated cells. Furthermore, despite the IκBα decrease at late times of infection, p50 did not translocate into the nucleus upon TNF-α treatment, and this was observed in two different cell lines, i.e., MeWo and MRC5. The coimmunoprecipitation assays performed with MeWo cells tended to show that VZV destabilizes p50 and thus reduces the occurrence of p65-p50 heterodimers, leading to an accumulation of p65 in the nuclei of infected cells independently of p50. It has been shown by ChIP assay that the *icam-1* promoter, in opposition to the *il-8* promoter, has less affinity for NF-κB dimers containing p50-independent p65 (51), explaining partly why the *il-8* promoter seemed less affected by the inhibitory effect of the infection, with the promoters with the most affinity for p50-independent complexes being the least inhibited by VZV.

Another observation that has to be highlighted is that VZV-induced nuclear NF-κB subunits did not bind a probe carrying the *icam-1* promoter NF-κB sequence in vitro, while they still slightly bound the NF-κB sequence present in the HIV LTR promoter. This could be correlated with a higher affinity of the VZV-induced nuclear NF-κB subunits for the LTR sequence than for the *icam-1* sequence. Furthermore, supershift assays were performed to identify the subunits binding to each of the probes used. Despite a slight presence of p52, it was shown that these two probes bound the same subunits in response to TNF-α, i.e., p50 and p65.

VZV also induced a strong nuclear accumulation of p52 in MeWo cells and, to a lesser extent, in MRC5 cells. This phenomenon has been described for other viruses, such as Epstein-Barr virus and human T-cell leukemia virus (9, 19, 44, 46), but never for an alphaherpesvirus. We have also reported for the first time an alphaherpesvirus-induced nuclear translocation of p100 in both melanoma cells and fibroblasts. Not

much is known about the mechanisms leading to the nuclear localization of p100, but its processing in the nucleus is IKKα dependent (48). The nuclear accumulation of p100 could very well play a role in the inhibition of NF-κB binding to cellular promoters. Indeed, p100 is one of the multiple NF-κB inhibitors containing ankyrin motifs, along with the IκBs and p105 (11, 16, 34). Furthermore, an increase in p100-associated p65 in VZV-infected MeWo total cell lysates was observed, and p100 also seemed to be more associated with p50 in total cell lysates, which could partly explain its cytoplasmic retention. Nevertheless, the coimmunoprecipitation of p100 with p65 in nuclear extracts of both mock- and VZV-infected cells was not feasible (data not shown). The mechanisms underlying the VZV-induced nuclear accumulation of p100, along with its possible consequences, are currently under investigation.

It was shown that VZV activates NF-κB in macrophages and HEK293 cells in a Toll-like receptor 2-dependent manner, leading to proinflammatory cytokine expression (57). In this work, the induction of TNF-α (data not shown), IL-6 (data not shown), and IL-8 mRNA expression in VZV-infected MeWo cells was shown. Nevertheless, IL-8 induction by the virus could not solely be explained by p65 recruitment to its promoter. Indeed, ChIP assay analysis showed that VZV did not increase p65 recruitment to this promoter.

Herpes simplex virus type 1, another alphaherpesvirus closely related to VZV, activates NF-κB via the IKK complex pathway and needs this activation to replicate properly (21, 47). It was recently shown that the NF-κB complex selectively activates the expression of viral genes, such as the ICP0 gene, and inhibits cellular ones. This inhibition is due to modifications of the chromatin structure in infected cells (6). We showed that VZV-induced NF-κB inhibition was not due to chromatin modifications at the promoter region, since histone H3 was still acetylated and HDAC3-containing complexes were removed. Nevertheless, while the shutoff does not seem to be due to acetylation inhibition or mRNA destabilization, we demonstrated in another study that the VZV immediate-early protein IE63 was able to interact with the transcription initiation complex and inhibit several cellular genes (10, 18). Furthermore, it has been shown for other NF-κB-dependent genes that to fully respond to NF-κB, the promoter must be derepressed by removal of a repressor complex containing p50 homodimers from the promoter region (27). Therefore, we postulate that the lower level of p50 at the promoters in VZV-infected cells could mean that this complex was removed by the infection, whereas no transcriptionally active heterodimers were recruited. Moreover, we also observed an inhibition of NF-κB recruitment in vitro by mobility shift assay, suggesting that it is probably a direct modification of the NF-κB dimer that is responsible for the inhibition. Besides, in the case of herpes simplex virus type 1, NF-κB was needed for virus replication, especially for ICP0 expression. The occurrence of functional NF-κB binding sites in the VZV genome has not been studied much, but it was recently shown that the intergenic region between *orf63* and *orf62* contains a nonfunctional one (32). It would be worth studying the replication and viral gene expression of VZV in cells unable to activate both NF-κB pathways. Nuclear NF-κB could either have a direct effect on viral promoter stimulation or an indirect effect by activating cellular factors that promote or slow down viral replication.

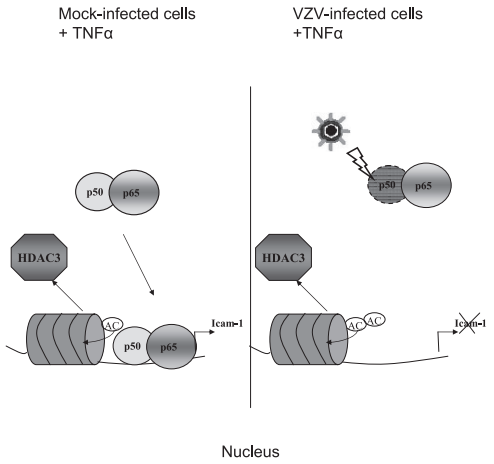

FIG. 10. VZV inhibits *icam-1* transcription upon TNF-α treatment by targeting p50-p65 heterodimers. VZV inhibits NF-κB recruitment to the *icam-1* promoter region and, to a lesser extent, to the *il-8* promoter after TNF-α treatment. Inhibition was observed both in vitro and in vivo, although VZV did not inhibit promoter acetylation but, on the contrary, enhanced it. VZV is able to inhibit NF-κB nuclear translocation by destabilizing p50. p65-p50 heterodimers are crucial for TNF-α induction of the *icam-1* gene, explaining why this gene is no longer induced.

Indeed, NF-κB is also involved in cell cycle progression, particularly by stimulating cyclin D1 expression (for a review, see reference 33). Also, CDK1 has been shown to greatly influence the localization and repressor activity of the VZV protein IE63 (22), and the use of the CDK1 inhibitor roscovitine significantly slows down VZV replication in MeWo cells (53).

Taken together, these results show that VZV is able to inhibit NF-κB nuclear translocation by destabilizing p50. Because p65-p50 heterodimers are crucial for TNF-α induction of the *icam-1* gene, this could explain why this gene is no longer induced despite correct acetylation of the promoter (Fig. 10). Therefore, it seems that VZV modulates several aspects of the immune response by modulating NF-κB nuclear shuttling and its recruitment to cellular promoters. NF-κB plays a central role in innate and adaptive immune responses. Its activation during early stages of viral infection leads to the expression of several immune response genes, such as those for proinflammatory cytokines (IFN-β, TNF-α, IL-6, and IL-8), chemokines (RANTES), and adhesion molecules (ICAM-1 and VCAM-1). NF-κB also strongly induces major histocompatibility complex class I and CD80/86 expression on antigen-presenting cells, thus increasing T-cell activation.

Regulating the actions of this transcription factor will lead to evident advantages for the control of infection progression, especially in melanocytes, which bear high viral replication loads in the skin.

ACKNOWLEDGMENTS

This work was supported by a grant from the National Fund for Scientific Research (FNRS, Brussels, Belgium).

N.E. is a Ph.D. student and teacher's assistant at the University of Liège, E.D. is a research associate at the FNRS, C.S.-D. is senior research associate at the University of Liège, and J.P. is a research director at the FNRS.

REFERENCES

1. **Abendroth, A., and A. Arvin.** 2000. Host response to primary infection, p. 142–156. *In* A. Arvin and A. Gershon (ed.), Varicella-zoster virus: virology and clinical management. Cambridge University Press, Cambridge, United Kingdom.
2. **Abendroth, A., I. Lin, B. Slobedman, H. Ploegh, and A. M. Arvin.** 2001. Varicella-zoster virus retains major histocompatibility complex class I proteins in the Golgi compartment of infected cells. J. Virol. **75:**4878–4888.
3. **Abendroth, A., G. Morrow, A. L. Cunningham, and B. Slobedman.** 2001. Varicella-zoster virus infection of human dendritic cells and transmission to T cells: implications for virus dissemination in the host. J. Virol. **75:**6183–6192.
4. **Abendroth, A., B. Slobedman, E. Lee, E. Mellins, M. Wallace, and A. M. Arvin.** 2000. Modulation of major histocompatibility class II protein expression by varicella-zoster virus. J. Virol. **74:**1900–1907.
5. **Amici, C., G. Belardo, A. Rossi, and M. G. Santoro.** 2001. Activation of I kappa B kinase by herpes simplex virus type 1. A novel target for antiherpetic therapy. J. Biol. Chem. **276:**28759–28766.
6. **Amici, C., A. Rossi, A. Costanzo, S. Ciafre, B. Marinari, M. Balsamo, M. Levrero, and M. G. Santoro.** 2006. Herpes simplex virus disrupts NF-kappaB regulation by blocking its recruitment on the IkappaBalpha promoter and directing the factor on viral genes. J. Biol. Chem. **281:**7110–7117.
7. **Arvin, A. M.** 1996. Varicella-zoster virus. Clin. Microbiol. Rev. **9:**361–381.
8. **Beinke, S., and S. C. Ley.** 2004. Functions of NF-kappaB1 and NF-kappaB2 in immune cell biology. Biochem. J. **382:**393–409.
9. **Beraud, C., S. C. Sun, P. Ganchi, D. W. Ballard, and W. C. Greene.** 1994. Human T-cell leukemia virus type I Tax associates with and is negatively regulated by the NF-kappa B2 p100 gene product: implications for viral latency. Mol. Cell. Biol. **14:**1374–1382.
10. **Bontems, S., E. Di Valentin, L. Baudoux, B. Rentier, C. Sadzot-Delvaux, and J. Piette.** 2002. Phosphorylation of varicella-zoster virus IE63 protein by casein kinases influences its cellular localization and gene regulation activity. J. Biol. Chem. **277:**21050–21060.
11. **Brown, K., S. Park, T. Kanno, G. Franzoso, and U. Siebenlist.** 1993. Mutual regulation of the transcriptional activator NF-kappa B and its inhibitor, I kappa B-alpha. Proc. Natl. Acad. Sci. USA **90:**2532–2536.
12. **Chen, J. J., Z. Zhu, A. A. Gershon, and M. D. Gershon.** 2004. Mannose 6-phosphate receptor dependence of varicella zoster virus infection in vitro and in the epidermis during varicella and zoster. Cell **119:**915–926.
13. **Croen, K. D., J. M. Ostrove, L. J. Dragovic, and S. E. Straus.** 1988. Patterns of gene expression and sites of latency in human nerve ganglia are different for varicella-zoster and herpes simplex viruses. Proc. Natl. Acad. Sci. USA **85:**9773–9777.
14. **Degitz, K., L. J. Li, and S. W. Caughman.** 1991. Cloning and characterization of the 5′-transcriptional regulatory region of the human intercellular adhesion molecule 1 gene. J. Biol. Chem. **266:**14024–14030.
15. **Dejardin, E.** 2006. The alternative NF-kappaB pathway from biochemistry to biology: pitfalls and promises for future drug development. Biochem. Pharmacol. **72:**1161–1179.
16. **Dejardin, E., G. Bonizzi, A. Bellahcene, V. Castronovo, M. P. Merville, and V. Bours.** 1995. Highly-expressed p100/p52 (NFKB2) sequesters other NF-kappa B-related proteins in the cytoplasm of human breast cancer cells. Oncogene **11:**1835–1841.
17. **Diamond, M. S., D. E. Staunton, S. D. Marlin, and T. A. Springer.** 1991. Binding of the integrin Mac-1 (CD11b/CD18) to the third immunoglobulin-like domain of ICAM-1 (CD54) and its regulation by glycosylation. Cell **65:**961–971.
18. **Di Valentin, E., S. Bontems, L. Habran, O. Jolois, N. Markine-Goriaynoff, A. Vanderplasschen, C. Sadzot-Delvaux, and J. Piette.** 2005. Varicella-zoster virus IE63 protein represses the basal transcription machinery by disorganizing the pre-initiation complex. Biol. Chem. **386:**255–267.
19. **Eliopoulos, A. G., J. H. Caamano, J. Flavell, G. M. Reynolds, P. G. Murray, J. L. Poyet, and L. S. Young.** 2003. Epstein-Barr virus-encoded latent infection membrane protein 1 regulates the processing of p100 NF-kappaB2 to p52 via an IKKgamma/NEMO-independent signalling pathway. Oncogene **22:**7557–7569.
20. **Gilden, D. H., Y. Rozenman, R. Murray, M. Devlin, and A. Vafai.** 1987. Detection of varicella-zoster virus nucleic acid in neurons of normal human thoracic ganglia. Ann. Neurol. **22:**377–380.
21. **Gregory, D., D. Hargett, D. Holmes, E. Money, and S. L. Bachenheimer.** 2004. Efficient replication by herpes simplex virus type 1 involves activation of the IκB kinase-IκB-p65 pathway. J. Virol. **78:**13582–13590.
22. **Habran, L., S. Bontems, E. Di Valentin, C. Sadzot-Delvaux, and J. Piette.** 2005. Varicella-zoster virus IE63 protein phosphorylation by roscovitine-sensitive cyclin-dependent kinases modulates its cellular localization and activity. J. Biol. Chem. **280:**29135–29143.
23. **Harson, R., and C. Grose.** 1995. Egress of varicella-zoster virus from the melanoma cell: a tropism for the melanocyte. J. Virol. **69:**4994–5010.
24. **Hata, A., L. Zerboni, M. Sommer, A. A. Kaspar, C. Clayberger, A. M. Krensky, and A. M. Arvin.** 2001. Granulysin blocks replication of varicella-zoster virus and triggers apoptosis of infected cells. Viral Immunol. **14:**125–133.
25. **Hayden, M. S., and S. Ghosh.** 2004. Signaling to NF-kappaB. Genes Dev. **18:**2195–2224.
26. **Herrero, J. A., P. Mathew, and C. V. Paya.** 1995. LMP-1 activates NF-kappa B by targeting the inhibitory molecule I kappa B alpha. J. Virol. **69:**2168–2174.
27. **Hoberg, J. E., F. Yeung, and M. W. Mayo.** 2004. SMRT derepression by the IkappaB kinase alpha: a prerequisite to NF-kappaB transcription and survival. Mol. Cell **16:**245–255.
28. **Hou, J., V. Baichwal, and Z. Cao.** 1994. Regulatory elements and transcription factors controlling basal and cytokine-induced expression of the gene encoding intercellular adhesion molecule 1. Proc. Natl. Acad. Sci. USA **91:**11641–11645.
29. **Ito, M., T. Nakano, T. Kamiya, K. Kitamura, T. Ihara, H. Kamiya, and M. Sakurai.** 1991. Effects of tumor necrosis factor alpha on replication of varicella-zoster virus. Antivir. Res. **15:**183–192.
30. **Jones, J. O., and A. M. Arvin.** 2006. Inhibition of the NF-κB pathway by varicella-zoster virus in vitro and in human epidermal cells in vivo. J. Virol. **80:**5113–5124.
31. **Jones, J. O., and A. M. Arvin.** 2005. Viral and cellular gene transcription in fibroblasts infected with small plaque mutants of varicella-zoster virus. Antivir. Res. **68:**56–65.
32. **Jones, J. O., M. Sommer, S. Stamatis, and A. M. Arvin.** 2006. Mutational analysis of the varicella-zoster virus ORF62/63 intergenic region. J. Virol. **80:**3116–3121.
33. **Joyce, D., C. Albanese, J. Steer, M. Fu, B. Bouzahzah, and R. G. Pestell.** 2001. NF-kappaB and cell-cycle regulation: the cyclin connection. Cytokine Growth Factor Rev. **12:**73–90.
34. **Kanno, T., G. Franzoso, and U. Siebenlist.** 1994. Human T-cell leukemia virus type I Tax-protein-mediated activation of NF-kappa B from p100 (NF-kappa B2)-inhibited cytoplasmic reservoirs. Proc. Natl. Acad. Sci. USA **91:**12634–12638.
35. **Karin, M., and Y. Ben-Neriah.** 2000. Phosphorylation meets ubiquitination: the control of NF-κB activity. Annu. Rev. Immunol. **18:**621–663.
36. **Koropchak, C. M., S. M. Solem, P. S. Diaz, and A. M. Arvin.** 1989. Investigation of varicella-zoster virus infection of lymphocytes by in situ hybridization. J. Virol. **63:**2392–2395.
37. **Kouskouti, A., and I. Talianidis.** 2005. Histone modifications defining active genes persist after transcriptional and mitotic inactivation. EMBO J. **24:**347–357.
38. **Ku, C. C., L. Zerboni, H. Ito, B. S. Graham, M. Wallace, and A. M. Arvin.** 2004. Varicella-zoster virus transfer to skin by T cells and modulation of viral replication by epidermal cell interferon-alpha. J. Exp. Med. **200:**917–925.
39. **Lebedeva, T., N. Anikeeva, S. A. Kalams, B. D. Walker, I. Gaidarov, J. H. Keen, and Y. Sykulev.** 2004. Major histocompatibility complex class I-intercellular adhesion molecule-1 association on the surface of target cells: implications for antigen presentation to cytotoxic T lymphocytes. Immunology **113:**460–471.
40. **Lebedeva, T., M. L. Dustin, and Y. Sykulev.** 2005. ICAM-1 co-stimulates target cells to facilitate antigen presentation. Curr. Opin. Immunol. **17:**251–258.
41. **Moffat, J. F., M. D. Stein, H. Kaneshima, and A. M. Arvin.** 1995. Tropism of varicella-zoster virus for human $CD4^+$ and $CD8^+$ T lymphocytes and epidermal cells in SCID-hu mice. J. Virol. **69:**5236–5242.
42. **Montag, C., J. Wagner, I. Gruska, and C. Hagemeier.** 2006. Human cytomegalovirus blocks tumor necrosis factor alpha- and interleukin-1β-mediated NF-κB signaling. J. Virol. **80:**11686–11698.
43. **Morrow, G., B. Slobedman, A. L. Cunningham, and A. Abendroth.** 2003. Varicella-zoster virus productively infects mature dendritic cells and alters their immune function. J. Virol. **77:**4950–4959.
44. **Munoz, E., and A. Israel.** 1995. Activation of NF-kappa B by the Tax protein of HTLV-1. Immunobiology **193:**128–136.
45. **Nikkels, A. F., C. Sadzot-Delvaux, and G. E. Pierard.** 2004. Absence of intercellular adhesion molecule 1 expression in varicella zoster virus-infected keratinocytes during herpes zoster: another immune evasion strategy? Am. J. Dermatopathol. **26:**27–32.
46. **Paine, E., R. I. Scheinman, A. S. Baldwin, Jr., and N. Raab-Traub.** 1995. Expression of LMP1 in epithelial cells leads to the activation of a select subset of NF-kappa B/Rel family proteins. J. Virol. **69:**4572–4576.
47. **Patel, A., J. Hanson, T. I. McLean, J. Olgiate, M. Hilton, W. E. Miller, and S. L. Bachenheimer.** 1998. Herpes simplex type 1 induction of persistent NF-kappa B nuclear translocation increases the efficiency of virus replication. Virology **247:**212–222.
48. **Qing, G., and G. Xiao.** 2005. Essential role of IkappaB kinase alpha in the constitutive processing of NF-kappaB2 p100. J. Biol. Chem. **280:**9765–9768.
49. **Rothlein, R., M. Czajkowski, M. M. O'Neill, S. D. Marlin, E. Mainolfi, and V. J. Merluzzi.** 1988. Induction of intercellular adhesion molecule 1 on primary and continuous cell lines by pro-inflammatory cytokines. Regulation by pharmacologic agents and neutralizing antibodies. J. Immunol. **141:**1665–1669.
50. **Sadzot-Delvaux, C., S. Debrus, A. Nikkels, J. Piette, and B. Rentier.** 1995.

Varicella-zoster virus latency in the adult rat is a useful model for human latent infection. Neurology **45:**S18–S20.

51. **Sasaki, C. Y., T. J. Barberi, P. Ghosh, and D. L. Longo.** 2005. Phosphorylation of RelA/p65 on serine 536 defines an IκBα-independent NF-κB pathway. J. Biol. Chem. **280:**34538–34547.
52. **Staunton, D. E., S. D. Marlin, C. Stratowa, M. L. Dustin, and T. A. Springer.** 1988. Primary structure of ICAM-1 demonstrates interaction between members of the immunoglobulin and integrin supergene families. Cell **52:**925–933.
53. **Taylor, S. L., P. R. Kinchington, A. Brooks, and J. F. Moffat.** 2004. Roscovitine, a cyclin-dependent kinase inhibitor, prevents replication of varicella-zoster virus. J. Virol. **78:**2853–2862.
54. **Torigo, S., T. Ihara, and H. Kamiya.** 2000. IL-12, IFN-gamma, and TNF-alpha released from mononuclear cells inhibit the spread of varicella-zoster virus at an early stage of varicella. Microbiol. Immunol. **44:**1027–1031.
55. **Volanti, C., J. Y. Matroule, and J. Piette.** 2002. Involvement of oxidative stress in NF-kappaB activation in endothelial cells treated by photodynamic therapy. Photochem. Photobiol. **75:**36–45.
56. **Voraberger, G., R. Schafer, and C. Stratowa.** 1991. Cloning of the human gene for intercellular adhesion molecule 1 and analysis of its 5′-regulatory region. Induction by cytokines and phorbol ester. J. Immunol. **147:**2777–2786.
57. **Wang, J. P., E. A. Kurt-Jones, O. S. Shin, M. D. Manchak, M. J. Levin, and R. W. Finberg.** 2005. Varicella-zoster virus activates inflammatory cytokines in human monocytes and macrophages via Toll-like receptor 2. J. Virol. **79:**12658–12666.
58. **Weller, T. H., and H. M. Witton.** 1958. The etiologic agents of varicella and herpes zoster; serologic studies with the viruses as propagated in vitro. J. Exp. Med. **108:**869–890.
59. **Zerboni, L., M. Sommer, C. F. Ware, and A. M. Arvin.** 2000. Varicella-zoster virus infection of a human CD4-positive T-cell line. Virology **270:**278–285.